EVTeC 2023
6th International Electric Vehicle Technology Conference 2023

20231078

Flux-based Cascade Vector Control for xEV Applications

- Reduction of Calibration Time for Torque Response -

Shun Taniguchi [1)] Kentaro Matsuo [2)] Kazuaki Tobari [1)]
Toshiyuki Ajima [1)] Kenichi Yoshida [2)] Eigo Kishimoto [2)]

1) Hitachi, Ltd., Hitachi-shi, Ibaraki, Japan
E-mail: shun.taniguchi.wu@hitachi.com
2) Hitachi Astemo, Ltd., Hitachinaka-shi, Ibaraki, Japan
E-mail: kentaro.matsuo.xb@hitachiastemo.com

ABSTRACT: Flux-based cascade vector control is proposed, which uses flux instead of current for torque control. The proposed method does not require any step-response test but instead employs a steady-state test for torque-response calibration. The method is verified by conducting an experiment using an EV motor. A reduction in calibration time is realized with precise torque control response.

KEY WORDS: permanent magnet synchronous motor, torque control, calibration time, magnetic saturation

1. INTRODUCTION

Permanent Magnet Synchronous Motors (PMSM) are applied to main traction motor for xEVs. The main traction motors for xEVs are required to reduce their size and weight because of the installation space and the magnetic saturation of their motors have been becoming larger. Along with it, modeling for motors with a magnetic saturation(1), design method for them(2), and motor control methods for them(3) have been proposed.

The authors proposed a cascade vector control that controls the inverter output voltage by using the inverse model of the motor(4). The control realizes stable control also at high speed region. However, if there are parameter errors in the inverse model, the current control response is different from the expected response. To reduce the variation of current response, the conventional method uses lookup tables of inductance. The tables need to be calibrated by a step-response test. The calibration of the response time by the step-response test is difficult because of current harmonics. In addition, the variation of speed by torque step makes the measurement errors.

To cope with this problem, this paper proposes flux-based cascade vector control. It uses flux instead of current for torque control. The proposed method is verified by conducting an experiment using an EV motor. The proposed method does not require any step-response test but instead employs a steady-state test for torque-response calibration. Therefore, a reduction in calibration time is realized with precise torque control response.

2. CONVENTIONAL METHOD

2.1. Constitution

Fig.1 shows the block diagram of motor drive system in this paper. Where T^* is torque reference, I_d^*, I_q^* are dq-axis current reference, V_d^*, V_q^* are dq-axis voltage reference, V_u^*, V_v^*, V_w^* are three phase voltage reference, V_{dc} is inverter DC voltage, I_u, I_v, I_w are three phase current, I_{uc}, I_{vc}, I_{wc} are detected three phase current, I_{dc}, I_{qc} are actual dq-axis current, θ is rotor angle, and ω_1 is rotor speed. The target of this paper is motor drive system which controls torque by using rotor angle sensor. The auto current regulator written in Fig.1 is the target controller in this paper. Fig.2 shows the block diagram of conventional current-based cascade vector control. Where I_d^{**}, I_q^{**} are 2nd dq-axis current reference, ω_c is cut-off frequency of current controller, s is differential operator, R_c is setting stator resistance, L_{dc}, L_{qc} are setting dq-axis inductance, and K_{ec} is setting magnetic flux. The conventional control generates the 2nd dq-axis current reference I_d^{**}, I_q^{**} based on the current by using integrator, and inputs them to the motor reverse model which outputs dq-axis voltage reference. Though there are two types of inductance , that is static inductance and dynamic inductance, the conventional control shown in Fig.1 does not consider their difference.

2.2. Consideration of magnetic saturation

The voltage equation of PMSM considering magnetic saturation is shown in Eq.(1).

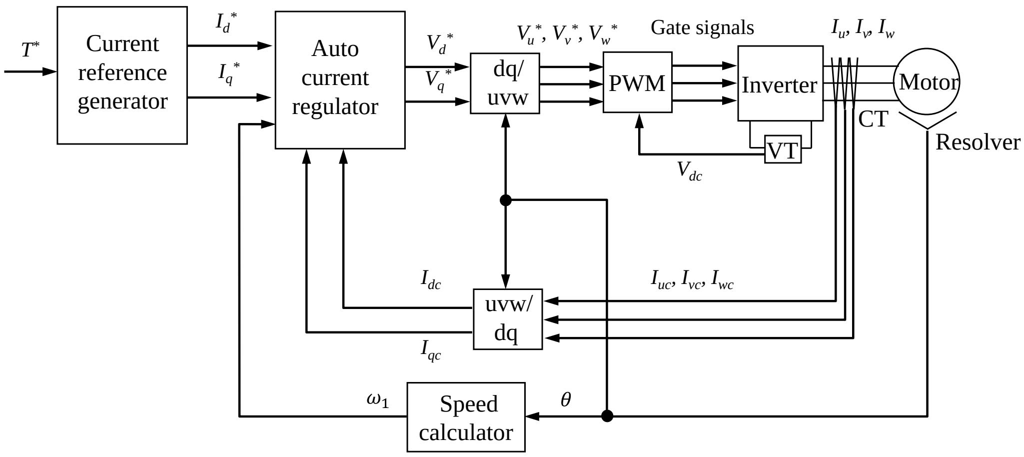

Fig. 1. Block diagram of motor drive system in this paper.

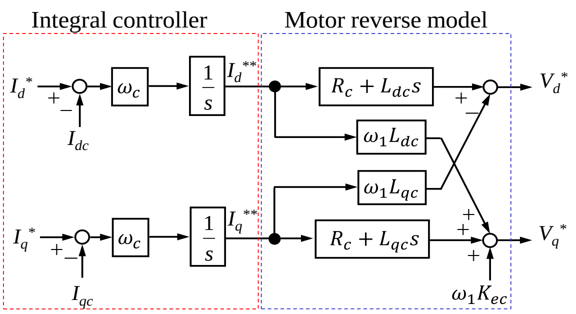

Fig. 2 Block diagram of current-based cascade vector control.

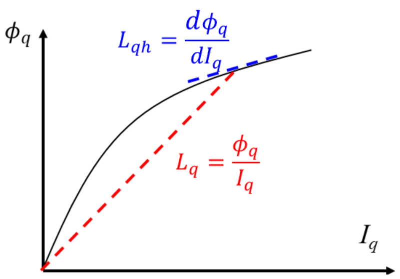

Fig. 3 Definition of dynamic and static inductance.

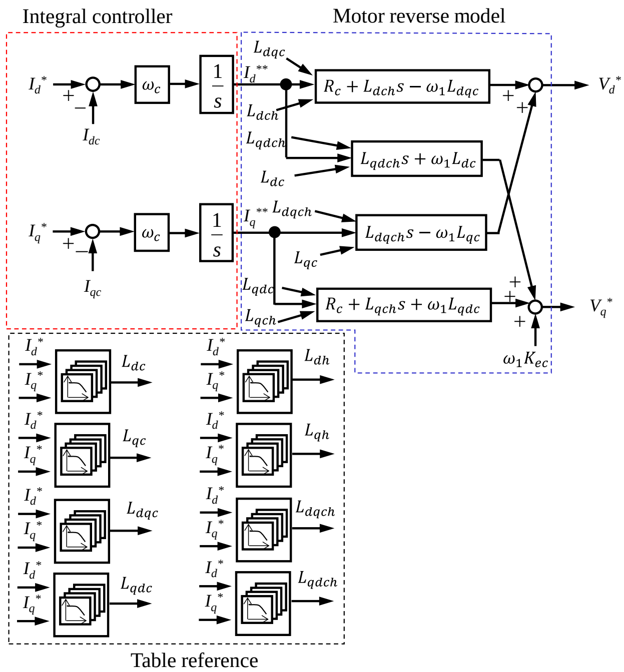

Fig. 4 Block diagram of current-based cascade vector control with consideration of magnetic saturation.

$$\begin{bmatrix} V_d \\ V_q \end{bmatrix} = \begin{bmatrix} R - \omega_1 L_{dq} & -\omega_1 L_q \\ \omega_1 L_d & R + \omega_1 L_{qd} \end{bmatrix} \begin{bmatrix} I_d \\ I_q \end{bmatrix} + \begin{bmatrix} L_{dh} & L_{dqh} \\ L_{qdh} & L_{qh} \end{bmatrix} s \begin{bmatrix} I_d \\ I_q \end{bmatrix} + \begin{bmatrix} 0 \\ \omega_1 K_e \end{bmatrix} \cdots\cdots\cdots\cdots (1)$$

Where V_d, V_q are dq-axis voltage, I_d, I_q are dq-axis current, R is stator resistance, L_d, L_q are dq-axis static inductance, L_{dq}, L_{qd} are mutual static inductance between dq axis, L_{dh}, L_{qh} are dq-axis dynamic inductance, L_{dqh}, L_{qdh} are mutual dynamic inductance between dq axis, K_e is magnetic flux.

The definition of dynamic and static inductance are shown in Fig.3. The dynamic inductance means a change of magnetic flux against current at the operation point. In contrast, the static inductance means a change of magnetic flux against current from 0A to the operation point. If the current-based cascade vector control considers Eq.(1), the block diagram in Fig.2 is changed as shown in Fig.4. This block diagram requires 8 look-up tables, which increases program size and calibration time. In addtion, step-response test is needed for the calibration of dynamic inductance.

3. PROPOSED METHOD

3.1. Constitution

The block diagram of the proposed flux-based cascade vector control is shown in Fig.5. Where φ_d^*, φ_q^* are dq-axis flux reference, φ_{dc}, φ_{qc} are estimated dq-axis flux, φ_d^{**}, φ_q^{**} are 2nd dq-axis flux reference. The proposed control calculates φ_d^*, φ_q^*, φ_{dc}, and φ_{qc} by refering to lookup tables, generates the 2nd dq-axis flux reference φ_d^{**}, φ_q^{**} by using integrator, and inputs them to the motor reverse model which outputs dq-axis voltage reference. The proposed

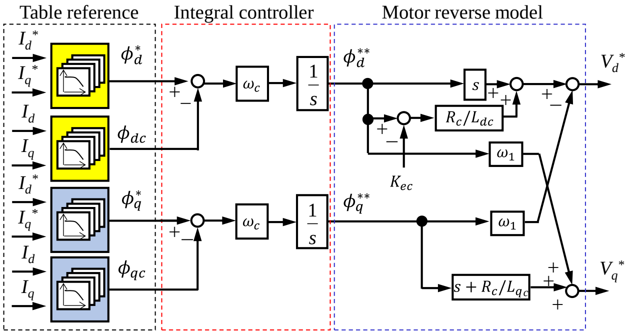

Fig. 5. Block diagram of flux-based cascade vector control.

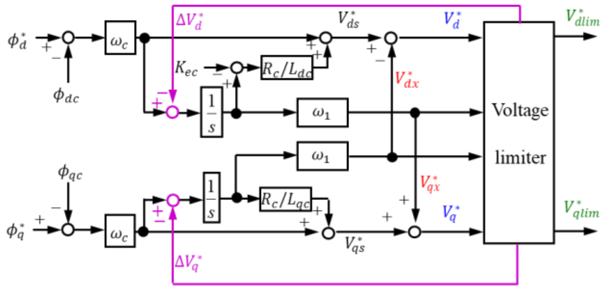

Fig. 6. Block diagram of the proposed flux-based cascade vector control considering voltage limiter.

method uses the flux for torque control instead of the current in conventional method. The principle of the proposed method is shown in the followings.

The voltage equation in Eq.(1) is changed as Eq.(2) by using flux instead of current.

$$\begin{bmatrix} V_d \\ V_q \end{bmatrix} = \frac{R}{L_d L_q - L_{dq} L_{qd}} \begin{bmatrix} L_q & -L_{qd} \\ -L_{dq} & L_d \end{bmatrix} \begin{bmatrix} \phi_d - K_e \\ \phi_q \end{bmatrix} + s \begin{bmatrix} \phi_d \\ \phi_q \end{bmatrix} + \omega_1 \begin{bmatrix} 0 & -1 \\ 1 & 0 \end{bmatrix} \begin{bmatrix} \phi_d \\ \phi_q \end{bmatrix} \cdots\cdots (2)$$

Assuming L_{qd} and L_{dq} are sufficiently smaller than L_d and L_q, Eq.(2) is changed as Eq.(3).

$$\begin{bmatrix} V_d \\ V_q \end{bmatrix} = \begin{bmatrix} \frac{R}{L_d} & 0 \\ 0 & \frac{R}{L_q} \end{bmatrix} \begin{bmatrix} \phi_d - K_e \\ \phi_q \end{bmatrix} + s \begin{bmatrix} \phi_d \\ \phi_q \end{bmatrix} + \omega_1 \begin{bmatrix} 0 & -1 \\ 1 & 0 \end{bmatrix} \begin{bmatrix} \phi_d \\ \phi_q \end{bmatrix} \cdots\cdots (3)$$

Eq.(3) can consider magnetic saturation of PMSM if φ_d, φ_q are changed according to current. On the other hand, all parameters (R, φ_d, φ_q, L_d, L_q, K_e) can be calibrated by a steady-state test.

3.2. Voltage Limiter

The block diagram of the proposed flux-based cascade vector control considering voltage limiter is shown in Fig.6. Where, V_{ds}^*, V_{qs}^* are direct components of dq-axis voltage reference, V_{dx}^*, V_{qx}^* are cross-coupling components of dq-axis voltage reference, V_{dlim}^*, V_{qlim}^* are limited dq-axis voltage reference, ΔV_d^*, ΔV_q^* are compensating components of dq-axis voltage reference.

Fig. 7 shows the voltage vectors of the proposed limiter. Because the cross-coupling components V_{dx}^*, V_{qx}^* correspond to the induced voltage terms, they are remained preferentially in order to keep stability. On the other hand, the direct components V_{ds}^*, V_{qs}^* correspond to the differential terms. The limit of the differential terms slows down the response of the torque control but does not destabilize the torque control. Since the excess voltage does not change the magnetic flux, the integrators are compensated by the excess voltage as shown in Fig.6.

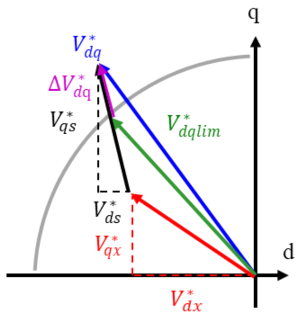

Fig. 7. Voltage vectors of the proposed limiter.

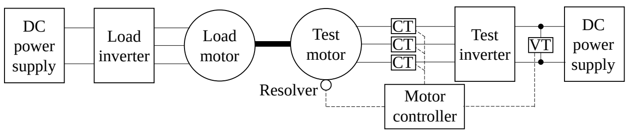

Fig. 8. Experimental system.

4. EXPERIMENTAL VERIFICATION

4.1. Experimental condition

The proposed method is verified by conducting an experiment of EV motor. Fig.8 shows the experimental system. The testing motor controller detects a rotor angle by using a resolver and controls testing motor. The load motor is controlled as its speed is constant. Time constant of step-response test (from zero to the setting torque) are measured at low speed (less than 1% of maximum speed) , at middle speed (30% of maximum speed), and at high speed (70% of maximum speed). Cut-off frequency of the proposed control is set 732 rad/s.

4.2. Experimental results

Fig.9 shows the rising results of step-response test from zero to maximum torque and Fig.10 shows the falling results of step-response test from maximum torque to zero. Regarding p.u. values, the maximum current of dq-axis current is defined as 1.0, the no-load flux is defined as 1.0, and the maximum torque is defined as 1.0. The time constants of each signal are as follows: d-axis current

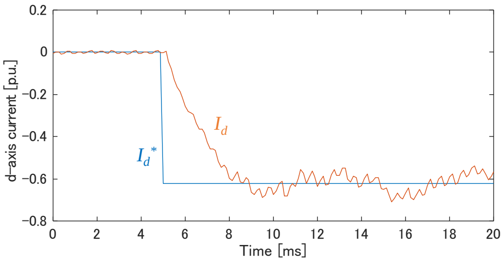

(a) d-axis current

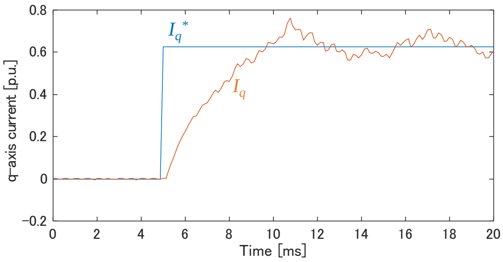

(b) q-axis current

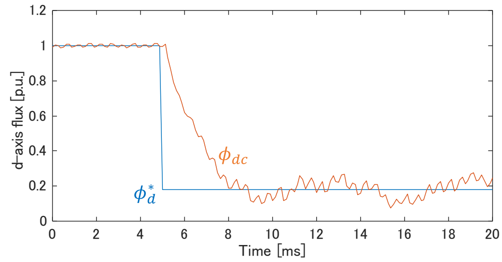

(c) d-axis flux

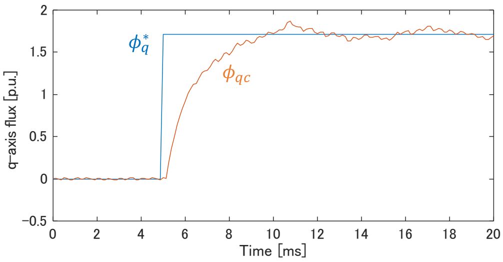

(d) q-axis flux

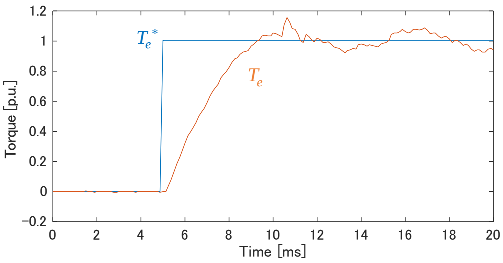

(e) torque

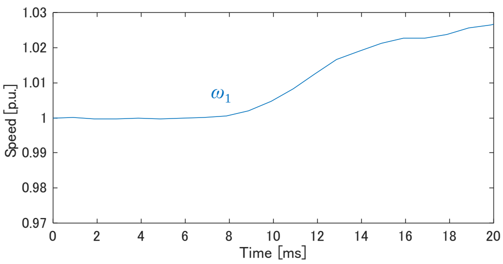

(f) speed

Fig.9 Experimental results with torque step rise from zero to maximum at middle speed.

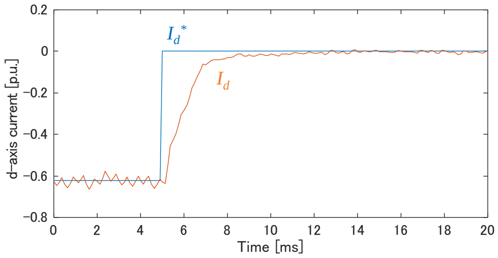

(a) d-axis current

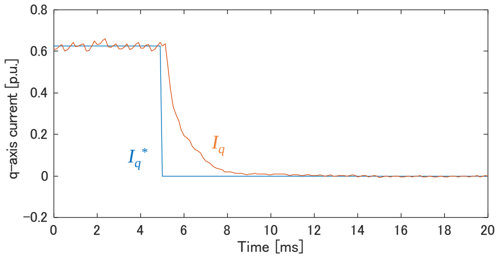

(b) q-axis current

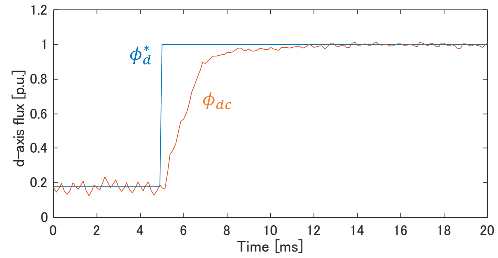

(c) d-axis flux

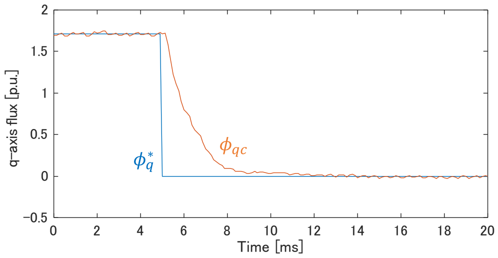

(d) q-axis flux

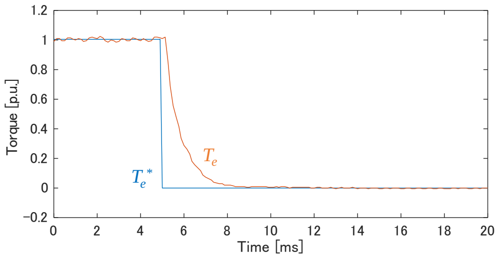

(e) torque

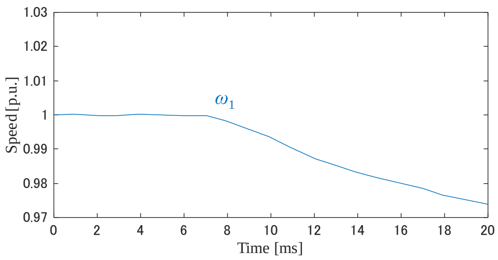

(f) speed

Fig.10 Experimental results with torque step rise from maximum to zero at middle speed.

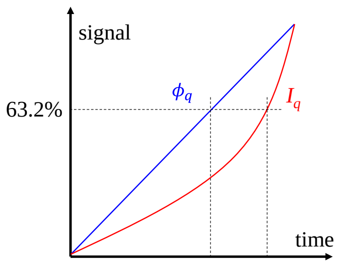

(a) flux-based control

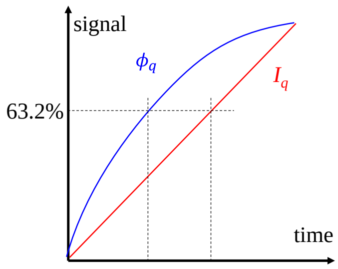

(b) current-based control

Fig. 11. Difference of control response between flux-based control and current-based cibtrol.

Table1 Experimental results of time constant [ms].

Speed	Label	Torque [p.u.]									
		1.0	0.8	0.6	0.4	0.2	-0.2	-0.4	-0.6	-0.8	-1.0
low	I_d	2.2	2.4	2.4	2.6	3.4	1.6	1.9	1.9	1.8	1.9
	I_q	2.5	2.2	2.1	2.0	1.8	1.7	2.0	2.1	2.4	2.6
	φ_d	1.9	2.2	2.2	2.5	2.9	1.5	1.9	1.8	1.6	1.8
	φ_q	1.7	1.6	1.6	1.8	1.8	1.6	1.8	1.6	1.8	1.6
	T	2.5	2.4	2.4	2.4	2.0	1.9	2.1	2.2	2.3	2.4
middle	I_d	2.1	2.1	2.2	1.9	1.9	3.0	2.6	2.0	2.1	2.1
	I_q	2.7	2.5	2.4	2.1	2.0	2.1	2.1	2.2	2.4	2.8
	φ_d	2.0	2.1	2.2	1.9	1.8	3.0	2.6	2.0	1.8	2.0
	φ_q	1.7	1.9	1.7	1.9	1.9	1.9	1.9	1.9	2.0	1.9
	T	2.6	2.5	2.4	2.4	2.0	2.4	2.4	2.4	2.5	2.6
high	I_d	-	-	1.6	2.0	1.5	1.7	1.7	1.7	-	-
	I_q	-	-	1.9	1.9	1.7	1.7	1.6	1.7	-	-
	φ_d	-	-	1.6	1.8	1.5	1.7	1.6	1.7	-	-
	φ_q	-	-	1.9	1.8	1.7	1.5	1.6	1.6	-	-
	T	-	-	2.1	2.2	1.7	1.7	1.9	2.2	-	-

is 2.1 ms, q-axis current is 2.7ms, d-axis flux is 2.0ms, q-axis flux is 1.7ms, and torque is 2.6ms at rise, and d-axis current is 1.5ms, q-axis current is 1.3ms, d-axis flux is 1.6ms, q-axis flux is 1.9ms, and torque is 1.1ms at fall. Though the expected time constant is about 1.4ms, the total expected time constant is about 1.7ms considering the control dead time 0.3ms. The time constants of dq-axis flux and d-axis current are within +/- 30 % from the expected time constant (1.2-2.2ms). On the other hand, q-axis current and torque rise slower than q-axis flux, and fall faster than q-axis flux.

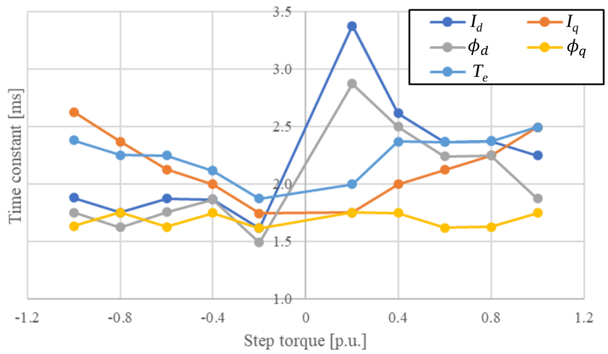

(a) low speed

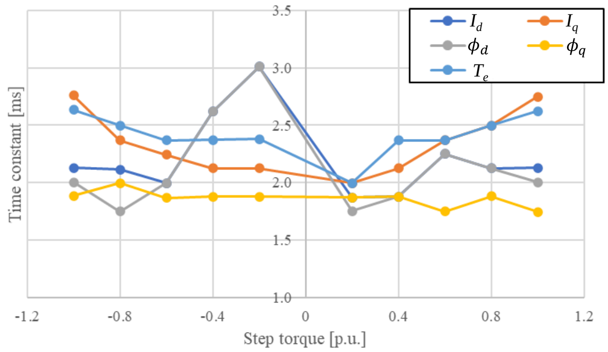

(b) middle speed

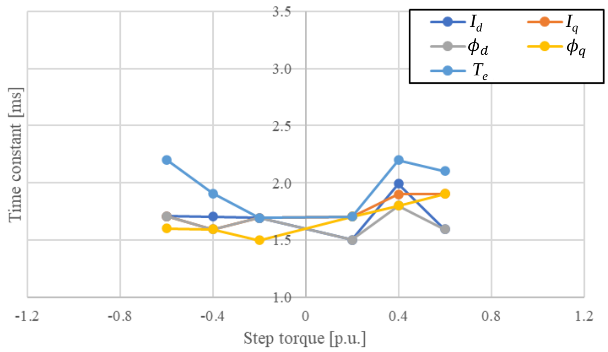

(c) high speed

Fig. 12. Experimental results of time constant.

The reason is that the current response is faster than the flux response when current is small, and it is slower than the flux response when current is large.That is, the response of current from 0 to 63.2% is slow at rise because the effect of low current region is dominant. On the contrary, the response of current from 100% to 36.8% is fast at fall because the effect of large current region is dominant. (Shown in Fig.11(a)) At the case of the conventional current-based cascade vector control, current operates as designed, and flux rises faster and falls slower. Regarding torque, the response depends on the rate of magnetic torque and reluctance torque. Because the magnetic torque is dominant at low and middle speed, the response of torque is similar to that of q-axis current. Because the reluctance torque is dominant at high speed, the response of torque is similar to that of dq-axis flux.

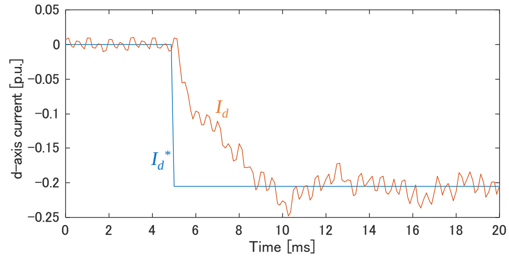

(a) d-axis current

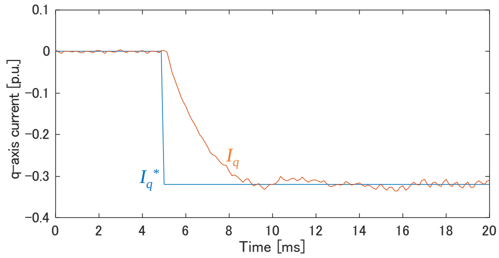

(b) q-axis current

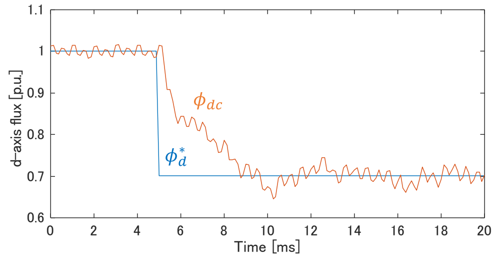

(c) d-axis flux

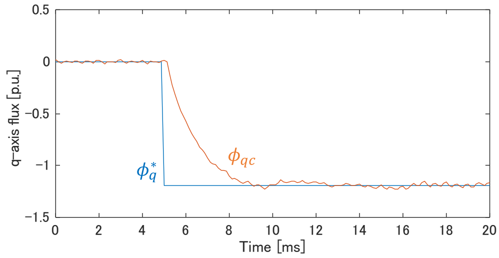

(d) q-axis flux

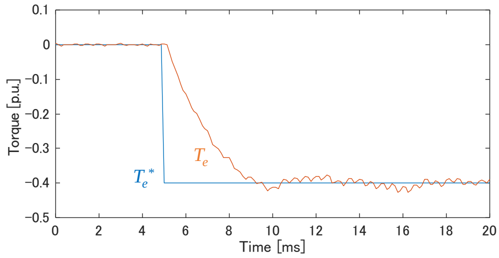

(e) torque

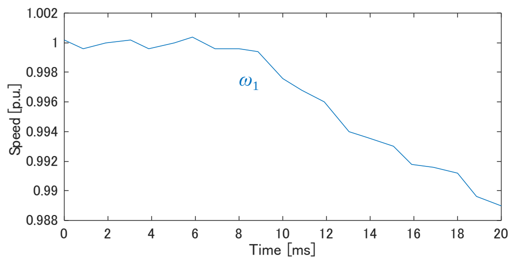

(f) speed

Fig.13 Experimental results with torque step rise from zero to -40% at middle speed.

Table 1 and Fig.12 shows experimental results of time constant. The yellow-marked cells in table 1 is out of the expected time constant (within +/- 30%, 1.2-2.2ms). The reason that their response except the green-marked cells is out of the expected time constant, is same as the results explained above. On the other hand, there are some region that the response of d-axis flux is slower than the expected response at low and middle speed as shown in the green-marked cells in Table 1. In order to analyze the reason, Fig.13 shows the experimental results with torque step rise from zero to -40% at middle speed. It can be seen from Fig.13(c), there are fluctuations of 200Hz in the d-axis flux at the step response. The reason of the fluctuations is considered to be voltage errors due to speed change. Because the testing motor controller uses low pass filter for speed, there is a gap between the controller's speed and actual speed.

5. CONCLUSION

This paper proposed the flux-based cascade vector control which can realize precise torque control considering magnet saturation with only steady-state calibration. The proposed method was verified that the error of the torque response is within 30%. If 30% of response error is allowed, the additional torque response calibration is not needed, which can reduce the calibration time of the motor controller.

REFERENCES

(1) J. Nakatsugawa, N. Iwasaki, H. Nagura, and Y. Iwaji : "Proposal of Mathematical Models Taking into Consideration Magnetic Saturation and Cross- Coupling Effects in Permanent Magnet Synchronous Motors", *IEEJ Trans. IA*, Vol.130, No.11, pp.1212-1220, 2010 (in Japanese)

(2) Y. Kano, T. Kosaka, N. Matsui and T. Nakanishi, "Design of Saliency-Based Sensorless Drive IPM Motors for General Industrial Applications," *2008 IEEE Industry Applications Society Annual Meeting*, pp. 1-6, 2008

(3) H.Nagura, Y.Iwaji, J.Nakatsugawa, N.Iwasaki : "New Vector Controller for PM Motors which Modeled the Cross-Coupling Magnetic Flux Saturation", *The 2010 International Power Electronics Conference -ECCE ASIA-*, pp. 1064-1070, 2010

(4) K. Tobari, T. Endo, Y. Iwaji, and Y. Ito: "Examination of New Vector Control System of Permanent Magnet Synchronous Motor for High-Speed Drives", *Electrical enginerring in Japan*, Vol. 176, Issue 4, pp. 61-72, 2011.